






C-band 120-Gb/s PAM-4 transmission over 50-km SSMF with improved weighted decision-feedback equalizer

JUNWEI ZHANG,^{1,2}  XIONG WU,¹  LIN SUN,^{1,3} JIE LIU,^{2,6} ALAN PAK TAO LAU,^{3,4} CHANGJIAN GUO,^{1,5,7}  SIYUAN YU,² AND CHAO LU^{1,3}

¹Photonics Research Center, Department of Electronic and Information Engineering, The Hong Kong Polytechnic University, Hong Kong, China

²State Key Laboratory of Optoelectronic Materials and Technologies, School of Electronics and Information Technology, Sun Yat-Sen University, Guangzhou 510006, China

³The Hong Kong Polytechnic University Shenzhen Research Institute, Shenzhen 518057, China

⁴Photonics Research Center, Department of Electrical Engineering, The Hong Kong Polytechnic University, Hong Kong, China

⁵South China Academy of Advanced Optoelectronics, South China Normal University, Guangzhou 510006, China

⁶liujie47@mail.sysu.edu.cn

⁷changjian.guo@coer-scnu.org

Abstract: An improved weighted decision-feedback equalizer (IWDFE) is adopted and experimentally demonstrated to mitigate chromatic dispersion (CD) induced power fading for C-band four-level pulse amplitude modulation (PAM-4) system. Based on a compressed sigmoid nonlinear function, the IWDFE is superior to the conventional DFE, rule-1 and rule-2 based WDFEs in reducing both the error propagation probability and percentage of errors. The IWDFE is combined with a feed-forward equalizer (FFE) to deal with both pre-cursor and post-cursor interference simultaneously. We also introduce 2nd-order polynomial nonlinear terms in both FFE and IWDFE at receiver side, constructing a nonlinear FFE-IWDFE (N-FFE-IWDFE) to simultaneously equalize both the CD-induced power fading and nonlinear distortions. Experimental results show that compared with nonlinear FFE-DFE (N-FFE-DFE), rule-1 and rule-2 based nonlinear FFE-WDFEs (N-FFE-WDFEs), the N-FFE-IWDFE can significantly reduce the bit error ratio (BER), which is close to that of the error-propagation-free N-FFE-DFE. By utilizing the N-FFE-IWDFE, 120-Gb/s PAM-4 transmission system over 50-km standard single-mode fiber (SSMF) is realized with the BER below 7% hard-decision forward error correction (HD-FEC) limit of 3.8×10^{-3} , achieving around 1.1-dB improvement of the receiver sensitivity over the N-FFE-DFE. To the best of our knowledge, this is the first time that an IWDFE is employed for C-band IM/DD optical transmission system.

© 2021 Optica Publishing Group under the terms of the [Optica Open Access Publishing Agreement](#)

1. Introduction

Propelled by the proliferation of bandwidth-hungry services, such as video streaming, cloud-based computing, data storage, virtual and augmented reality, the ongoing growth of data center traffic drives the demand for high-speed signal transmission operating at 100 Gb/s and beyond. Owing to the characteristics of low cost, low power consumption and small footprint, intensity modulation and direct detection (IM/DD) scheme is an attractive solution for optical data center interconnections and access networks [1–4]. In order to transmit higher capacities with limited system bandwidth, spectrally efficient modulations such as four-level pulse amplitude modulation (PAM-4), carrier-less amplitude and phase modulation (CAP) and discrete multi-tone (DMT) have been extensively investigated in IM/DD systems [3,4]. Among those modulation formats,

PAM-4 can offer a better compromise between performance and computational complexity, which has been chosen as a standard format in 400G Ethernet with 8-lane \times 50-Gb/s and is a promising solution for the next-generation 800-G Ethernet with 8-lane \times 100-Gb/s [5–7].

Nevertheless, the transmission distance of high-speed PAM-4 systems operating in C-band is limited by the chromatic dispersion (CD), which results in severe power fading and nonlinear distortions of the received signal after square-law detection [8–12]. The nonlinear distortions can be effectively compensated by the Volterra nonlinear equalizers or their low-complexity versions [11,12]. Different from nonlinear distortions, the CD-induced power fading results in spectral nulls of the received signal spectrum, depending on the transmission distance and signal bandwidth [10]. To eliminate the CD induced power fading, optical dispersion compensation module [13], single-sideband or vestigial-sideband (SSB/VSB) modulation [14,15], CD pre-compensation [16], and Kramers-Kronig receiver [17,18] have been implemented. However, these schemes rely on either complicated system configurations or additional expensive devices, which might increase the system cost.

In contrast to CD compensation techniques using complicated system structures, digital signal processing (DSP) based CD compensation techniques can keep the IM/DD system flexible and cost effective, which are more attractive to be used to improve CD tolerance and extend transmission distance. According to [10], the receiver-side decision feedback equalizer (DFE) can effectively equalize the spectral nulls caused by CD-induced power fading. Meanwhile, a combination of a feed-forward equalizer (FFE) and a DFE is regarded as the best choice for the equalization of both pre-cursor and post-cursor interference [10]. The DFE equalizer has been applied along with a 3rd-order polynomial nonlinear equalizer (PNLE) in [19] to compensate the CD-induced power fading and nonlinear distortions in a C-band 56-Gb/s PAM-4 transmission over 80 km standard single-mode fiber (SSMF). Moreover, H. Xin et al. employed a joint Volterra-based FFE and Volterra-based DFE to mitigate the signal distortions and demonstrated C-band PAM-4 transmissions of 56 Gb/s over 60-km and 60 Gb/s over 80-km, respectively [20]. However, a main drawback of DFE is that it suffers from error propagation, which results in degradation of the system performance. To avoid error propagation, the transmitter-side Tomlinson-Harashima pre-coding (THP) [10] has been introduced to address the CD-induced power fading in IM/DD systems. By adopting the THP and Volterra FFE, Q. Hu et al. achieved C-band 56-Gb/s PAM-4 signal transmission over 80-km SSMF [21]. In [22], C-band 107-Gb/s PAM-4 transmission over 40-km SSMF has been experimentally demonstrated by using nonlinear THP and Volterra FFE. Nevertheless, THP suffers from a pre-coding loss and requires precise channel feedback [10,23]. Recently, a multi-symbol joint decision scheme with FFE-DFE was proposed and demonstrated in a C-band 112-Gb/s PAM-4 transmission system over 20-km SSMF to mitigate symbol error propagation and correct previous error symbols, at the expense of high computational complexity [8]. In addition, maximum likelihood sequence estimation (MLSE) based post filtering has been employed to whiten the colored noise after performing PNLE and FFE-DFE, constructing an adaptive channel-matched detection (ACMD) and realizing 64-Gb/s on-off keying (OOK) transmission over 100-km SSMF [24]. To relieve the equalization complexity, the MLSE was replaced with a fixed-state log-maximum a posteriori (log-MAP) detection in ACMD [25], achieving C-band 72-Gb/s OOK transmission over 100 km SSMF. Meanwhile, weighted DFE (WDFE) has been introduced to mitigate the burst-error propagation in a field-trial C-band 72-Gb/s OOK system over 18.8-km submarine optical cable [26]. However, multiple cascaded equalization including 3rd-order PNLE, FFE-WDFE and 2¹⁴-state MLSE was required, thus dramatically increasing implementation complexity and cost. Increasing transmission capacity and extending transmission distance are two hot topics in C-band dispersion-uncompensated IM/DD transmission research. Table 1 summarizes the current researches for C-band dispersion-uncompensated IM/DD transmission systems in terms of capacity, transmission distance and capacity–distance product.

Table 1. Current researches for C-band dispersion-uncompensated IM/DD transmission systems with BERs below 7% HD-FEC limit.

Reference	Capacity (Gb/s)	Distance (km)	Capacity–distance product	Modulation format
[8]	112	20	2.24	PAM-4
[10]	56	75	4.2	PAM-4
[19]	56	80	4.48	PAM-4
[20]	56	60	3.36	PAM-4
[21]	56	80	4.48	PAM-4
[22]	107	40	4.28	PAM-4
[22]	84	80	6.72	PAM-4
[24]	64	100	6.4	OOK
[25]	72	100	7.2	OOK
[26]	72	18.8	1.35	OOK
This work	120	50	6	PAM-4

In this paper, in order to improve the equalization performance and reduce the error propagation probability of conventional DFE, here we adopt and experimentally demonstrate a compressed sigmoid nonlinear function based improved WDFE (IWDFE) for C-band PAM-4 system with negligible increase in computational complexity. The IWDFE scheme is comparatively evaluated with two existing WDFE schemes, entitled ‘rule-1’ and ‘rule-2’ based WDFEs [27,28] as well as conventional DFE scheme in a PAM-4 transmission system. To simultaneously compensate both the CD-induced power fading and nonlinear distortions, 2nd-order polynomial nonlinear terms are introduced in FFE-IWDFE, FFE-WDFEs and FFE-DFE at receiver side, constructing nonlinear FFE-IWDFE (N-FFE-IWDFE), nonlinear FFE-WDFEs (N-FFE-WDFEs) and nonlinear FFE-DFE (N-FFE-DFE), respectively. Experimental results show that the conventional N-FFE-DFE outperforms the rule-1 and rule-2 based N-FFE-WDFEs since higher percentage of symbol errors are aroused by rule-1 and rule-2 schemes. Compared with N-FFE-DFE, rule-1 and rule-2 based N-FFE-WDFEs, the N-FFE-IWDFE can significantly reduce the bit error ratio (BER) thanks to the significant reduction of both error propagation probability and percentage of errors. Moreover, the achieved BER of the N-FFE-IWDFE is close to that of the error-propagation free (EP-free) N-FFE-DFE. Based on the N-FFE-IWDFE, 120-Gb/s PAM-4 transmission over 50-km SSMF is realized with a BER below 7% hard-decision forward error correction (HD-FEC) limit of 3.8×10^{-3} , achieving around 1.1-dB improvement of the receiver sensitivity over the N-FFE-DFE. To the best of our knowledge, this is the first time that an IWDFE is applied to reduce both the error propagation probability and percentage of errors in decision feedback equalization for C-band IM/DD optical transmission system.

2. Principle of the improved weighted decision-feedback equalizer

2.1. Improved weighted decision-feedback equalizer (IWDFE)

To mitigate both the CD-induced power fading and inter-symbol interference in IM/DD systems, linear FFE-DFE can be implemented as a post-equalizer at the receiver side. The n^{th} sample of the output of the FFE-DFE can be expressed as

$$y(n) = \sum_{k=0}^{N_1-1} h_1(k)x(n-k) + \sum_{k=1}^{D_1} w_1(k)\hat{y}(n-k) \quad (1)$$

where $x(n)$ is the n^{th} sample of the received signal, $h_1(w_1)$ and $N_1(D_1)$ are the kernel and memory length for the FFE (DFE), respectively. $\hat{y}(n)$ is the hard-decision output and feedback symbol of the DFE.

Since the FFE-DFE suffers from error propagation and degrades the system performance, it is feasible to use a soft decision based on weighted decisions to avoid the error propagation [27,28]. Here an IWDFE is introduced for PAM-based IM/DD systems after FFE, forming an FFE-IWDFE structure. The n^{th} sample of the output of the FFE-IWDFE can be expressed as

$$y(n) = \sum_{k=0}^{N_1-1} h_1(k)x(n-k) + \sum_{k=1}^{D_1} w_1(k)\tilde{y}(n-k) \quad (2)$$

where the soft-decision feedback symbol $\tilde{y}(n)$ is a combination of the output $y(n)$ and the hard-decision output $\hat{y}(n)$. The schematic diagram of the FFE-IWDFE is illustrated in Fig. 1. Compared with FFE-DFE, two new blocks including the reliability block and use block are added in FFE-IWDFE after symbol decision. The reliability block calculates a reliability value γ_n for each DFE output $y(n)$, which is similar with a likelihood measurement. Then the reliability use block uses this value in such a way to minimize the effect of error propagation [27,28]. The feedback symbol (i.e., soft decision output of the use block) $\tilde{y}(n)$ can be expressed as

$$\tilde{y}(n) = f(\gamma_n)\hat{y}(n) + [1 - f(\gamma_n)]y(n) = y(n) + f(\gamma_n)[\hat{y}(n) - y(n)] \quad (3)$$

where $f(\cdot)$ is the function that specifies the kind of reliability to be used. When $f(\gamma_n)$ is equal to 1, the IWDFE becomes a classical DFE. Whereas when $f(\gamma_n)$ is equal to 0, the IWDFE can be considered as an infinite impulse response (IIR) filter.

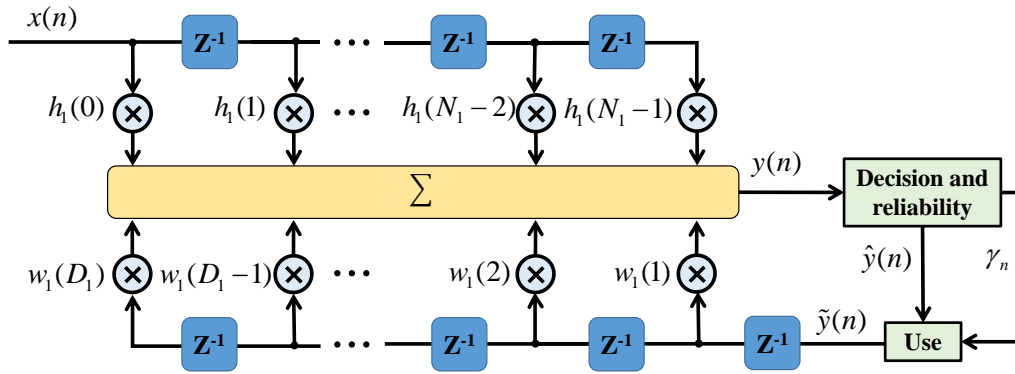


Fig. 1. Schematic diagram of the FFE-IWDFE.

2.2. Reliability calculation for PAM-4 constellation

The computation of the reliability, which is in the core of the IWDFE, depends on the specific constellation. Figure 2 depicts the calculation of reliability value γ_n for PAM-4 constellation. When the input symbol $y(n)$ (red solid circle) of the reliability block is between -3 and 3 , the reliability value γ_n can be calculated by

$$\gamma_n = 1 - |y(n) - \hat{y}(n)| \quad (4)$$

Therefore, when the input symbol $y(n)$ of the reliability block is close to the constellation point (i.e., hard decision point), the reliability value γ_n is close to 1. Moreover, when input symbol

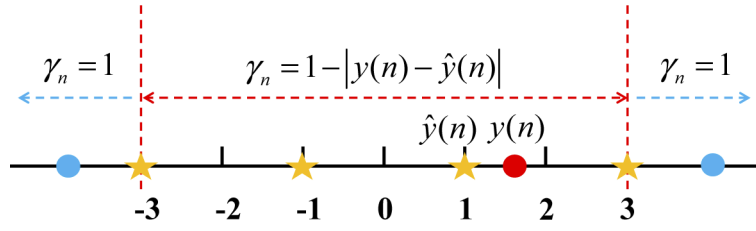


Fig. 2. Reliability calculation for PAM-4 constellation.

$y(n)$ (blue solid circle) of the reliability block is less than -3 or larger than 3 , the reliability value γ_n is equal to 1 . It should be noted that the reliability calculation can be extended to higher-level PAM constellation.

2.3. Reliability use of IWDFE

In order to increase the effect of reliability value γ_n when it is a high value as well as decrease this effect when it is a low value, an improved rule is performed for the IWDFE. The improved rule of IWDFE is based on a compressed sigmoid nonlinear function [28], which is corrected and can be expressed as

$$f(x) = \frac{1}{2} \left(\frac{1 - \exp \left[-a \left(\frac{x}{b} - 1 \right) \right]}{1 + \exp \left[-a \left(\frac{x}{b} - 1 \right) \right]} + 1 \right) \quad (5)$$

where a is a positive integer and b with $0 < b \leq 1$ is a compression factor. The parameters a and b are required to be optimized before performing the equalization with FFE-IWDFE. Once the pre-look-up table related to parameter a and b is obtained, we can directly use the pre-look-up table to map the input x to the output $f(x)$.

In addition to IWDFE, the equalization performance of the rule-1 and rule-2 based WDFEs [27,28] will also be evaluated and compared. The function $f(\cdot)$ of rule-1 based WDFE can be given by [27,28]

$$f_{\text{Rule-1}}(x) = \begin{cases} 1, & x = |y(n) - \hat{y}(n)| < d_{\min} \\ 0, & x = |y(n) - \hat{y}(n)| \geq d_{\min} \end{cases} \quad (6)$$

where d_{\min} with $0 \leq d_{\min} \leq 1$ is a threshold constant. Besides, the function $f(\cdot)$ of rule-2 based WDFE can be written as [27,28]

$$f_{\text{Rule-2}}(x) = \gamma_n \quad (7)$$

The abovementioned three $f(\cdot)$ functions of rule 1, rule 2 and improved rule are shown in Fig. 3 for comparison. d_{\min} is set to 0.5 for rule 1. It can be seen that the compressed sigmoid function is a good compromise between the threshold function and identity function, which improves the effect of the reliability value at a large γ_n and decrease this effect at a small γ_n . Moreover, the parameters a and b contribute greatly to the slope and width of compressed sigmoid nonlinear function of the improved rule. The detailed analyses of error propagation probability and equalization performance among these WDFEs will be presented in section 4.

The computational complexity of the equalizer can be quantified by the number of real-valued multiplications. Compared with conventional FFE-DFE based on Eq. (1), the FFE-IWDFE based on Eqs. (2)–(5) only requires additional one real-valued multiplication to obtain the feedback symbol, which is negligible.

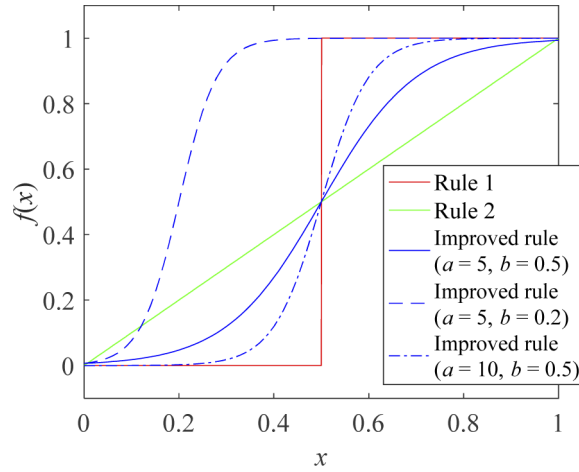


Fig. 3. $f(\cdot)$ function comparison for different rules.

2.4. Nonlinearity-aware improved weighted decision-feedback equalizer

Besides CD-induced power fading, the nonlinear distortions caused by the square-law detection should also be considered. Therefore, the 2nd-order polynomial nonlinear terms are introduced in the FFE-IWDFE, constructing an N-FFE-IWDFE. The n^{th} sample of the output of the N-FFE-IWDFE can be expressed as

$$y(n) = \sum_{k=0}^{N_1-1} h_1(k)x(n-k) + \sum_{k=0}^{N_2-1} h_2(k)x^2(n-k) + \sum_{k=1}^{D_1} w_1(k)\tilde{y}(n-k) + \sum_{k=1}^{D_2} w_2(k)\tilde{y}^2(n-k) \quad (8)$$

where h_2 (w_2) and N_2 (D_2) are the nonlinear kernel and memory length of the 2nd-order nonlinear terms of the N-FFE-IWDFE, respectively. The kernel coefficients can be obtained via training according to a recursive least squares (RLS) algorithm [29].

3. Experimental setup

The performance of the N-FFE-IWDFE was evaluated in a C-band 120-Gb/s PAM-4 based transmission system over 50-km SSMF. The experimental setup and DSP block diagram are illustrated in Fig. 4(a). At the transmitter, Gray-coded PAM-4 symbols were generated offline and simply pulse shaped by a rectangular filter with 2 samples per symbol. Then the resulted PAM-4 signal was loaded into an arbitrary waveform generator (AWG, Keysight M8194A) at a sample rate of 120-GSa/s to generate 60-GBaud PAM-4 electrical signal. After that, the 60-GBaud PAM-4 electrical signal from AWG was amplified by a linear electrical amplifier (EA, SHF S807) and then fed into a Mach-Zehnder modulator (MZM, FTM 7938EZ) for double side-band (DSB) electrical-optical conversion. The DC bias was set to the orthogonal point of around 4.2V and the measured modulation curve of the used MZM was depicted in Fig. 4(b). The peak-to-peak signal amplitude after EA and half-wave voltage of MZM were around 2.7 V and 5.2 V, respectively, which corresponds to a modulation depth of around 52%. The optical source was generated from an external cavity laser (ECL) with a center wavelength of 1550.12 nm. The launch power was around 4.1 dBm. After 50-km of SSMF transmission without any dispersion compensation, a variable optical attenuator (VOA) with an insertion loss of around 4.5 dB was employed to adjust the received optical power (ROP) of the received signal which was then detected by using a 70-GHz photo detector (PD). Note that an Erbium doped fiber amplifier (EDFA) was applied to boost the power up to 7 dBm due to the lack of a trans-impedance amplifier (TIA).

The detected electrical PAM-4 signal was digitized via a digital storage oscilloscope (DSO, Keysight UXR0804A) operating at a sample rate of 256 GSa/s. Finally, off-line DSP procedures including resampling, synchronization, equalization with half-symbol-spaced nonlinear FFE and symbol-spaced nonlinear IWDFE, PAM demodulation and error counting were performed. In this work, each data frame comprised 2^{17} PAM-4 symbols, in which the first 10000 PAM-4 symbols were utilized for the training process and the remaining symbols were effective data symbols. The BERs were evaluated by 5 data frames.

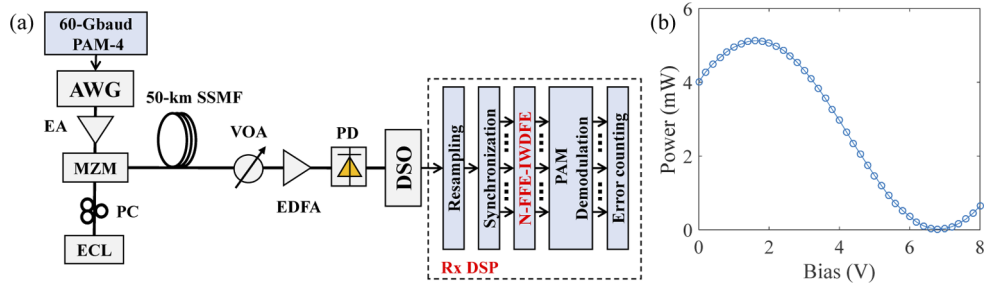


Fig. 4. (a) Experimental setup of the 120-Gb/s PAM-4 IM/DD system using N-FFE-IWDFE; (b) measured modulation curve of the used MZM. AWG: arbitrary waveform generator; EA: electrical amplifier; MZM: Mach-Zehnder modulator; ECL: external cavity laser; PC: polarization controller; SSMF: standard single-mode fiber; VOA: variable optical attenuator; PD: photo detector; DSO: digital storage oscilloscope.

4. Results and analysis

We firstly optimized the linear and nonlinear memory lengths of both the FFE and DFE parts of the N-FFE-DFE and N-FFE-WDFEs at a received optical power (ROP) of -10.5 dBm. For convenience, the optimization is based on the BER results of EP-free N-FFE-DFE, which can be regarded as a benchmark of the corresponding N-FFE-DFE and N-FFE-WDFEs. Figure 5(a) shows the measured BER versus the linear memory length N_1 at different linear memory length D_1 for EP-free FFE-DFE (i.e., the linear parts of the abovementioned equalizers). One can see that the BER performance of the EP-free FFE-DFE is improved as the memory length N_1 or D_1 increases. The improvement becomes negligible when the memory length $N_1 > 102$ and $D_1 > 34$. Then we optimize the nonlinear memory lengths N_2 and D_2 for the EP-free N-FFE-DFE with $N_1 = 102$ and $D_1 = 34$. The measured BER as a function of the nonlinear memory length N_2 at different nonlinear memory length D_2 is shown in Fig. 5(b). Compared with EP-free FFE-DFE, the BERs of EP-free N-FFE-DFE are significantly reduced. The best BER performance can be achieved when its nonlinear memory lengths approach $N_2 = 98$ and $D_2 = 24$. To balance the performance and complexity, $N_1 = 102$, $N_2 = 98$, $D_1 = 34$, and $D_2 = 24$ are set for the N-FFE-DFE and N-FFE-WDFEs in our experiment.

We then compared the equalization performance of different DFE and WDFEs. Different from the rule-2 based WDFE, the parameters d_{\min} of rule-1 based WDFE as well as a and b of IWDFE are required to be optimized. The measured BER as a function of threshold constant d_{\min} for rule-1 based N-FFE-WDFE is shown in Fig. 6(a). The BER results of EP-free N-FFE-DFE, N-FFE-DFE and rule-2 based N-FFE-WDFE are also included in Fig. 6(a). One can see that the rule-1 based N-FFE-WDFE achieves the best BER performance at $d_{\min} = 0$. In this case, the rule-1 based N-FFE-WDFE becomes a N-FFE-DFE since the reliability value γ_n is always equal to 1 when $d_{\min} = 0$. For comparison, we set $d_{\min} = 0.5$ for rule-1 based N-FFE-WDFE in the following experiment. In addition, the BER performance of rule-2 based N-FFE-WDFE is slightly worse than that of the N-FFE-DFE as expected [26]. The measured BER versus the compression factor

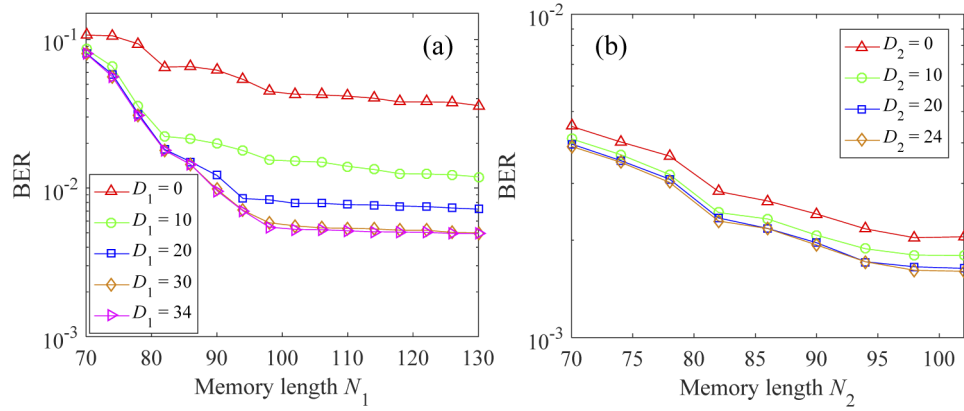


Fig. 5. (a) Measured BER versus memory length N_1 at different linear memory length D_1 for EP-free FFE-DFE; (b) measured BER versus memory length N_2 at different nonlinear memory length D_2 for EP-free N-FFE-DFE with $N_1 = 102$ and $D_1 = 34$. All results are measured after 50-km SSMF transmission at a ROP of -10.5 dBm.

b for N-FFE-IWDFE at different parameter a is presented in Fig. 6(b). It can be seen that the value of parameter a of N-FFE-IWDFE has little impact on the BER performance when the compression factor b is less than 0.3. Furthermore, the best BER achieved by the N-FFE-IWDFE at $a = 3$ and $b = 0.15$ is 2.176×10^{-3} , which is reduced by around half compared with those of the N-FFE-DFE and rule-1 and rule-2 based N-FFE-WDFEs. Meanwhile, the achieved BER of the N-FFE-IWDFE is also close to 1.615×10^{-3} achieved by EP-free N-FFE-DFE, which determines the lower bound for equalizers' BER performance [10]. Thus $a = 3$ and $b = 0.15$ are set for the N-FFE-IWDFE. It is noted that a high tolerance for the mapping error of $f(x)$ can be achieved for N-FFE-IWDFE due to the fact that the achieved BER is insensitive to the values of parameters a and b within a wide range.

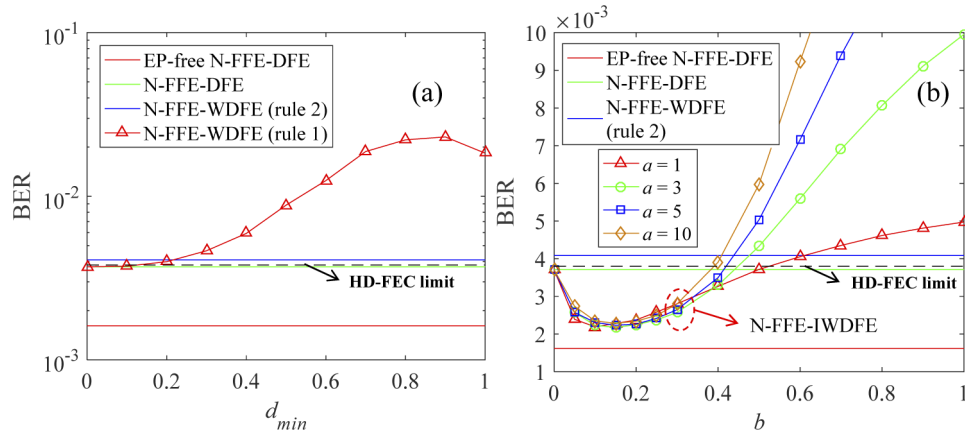


Fig. 6. (a) Measured BER as a function of threshold constant d_{\min} for rule-1 based N-FFE-WDFE; (b) measured BER as a function of compression factor b for N-FFE-IWDFE. All results are measured after 50-km SSMF transmission at a ROP of -10.5 dBm.

The error propagation probability and the length of burst consecutive errors using different DFEs were also evaluated after 50-km SSMF transmission at a ROP of -10.5 dBm. The probability mass function of the length of burst consecutive errors is shown in Fig. 7. The

following observations could be made from Fig. 7: 1) The maximum lengths of burst consecutive errors are the same as 9 for N-FFE-DFE and rule-1 based N-FFE-WDFE with $d_{\min} = 0.5$, but the latter suffers from higher percentage of symbol errors. 2) Due to decrease in the error propagation probability, the maximum lengths of burst consecutive errors are reduced to 4 and 2 by using rule-2 based N-FFE-WDFE and N-FFE-IWDFE, respectively. 3) The BER performance of rule-2 based N-FFE-WDFE is slightly worse than that of N-FFE-DFE as presented in Fig. 6, which is attributed to its higher percentage of single-symbol errors. 4) As can be seen from the inset, the probability of correct symbol decision (i.e., the length of the error burst is 0) for the N-FFE-IWDFE is the highest among all abovementioned equalizers thanks to its superior decision rule and significant decrease in the error propagation probability. 5) In conclusion, the IWDFE has the best performance on both the suppression of burst-error propagation and symbol decision.

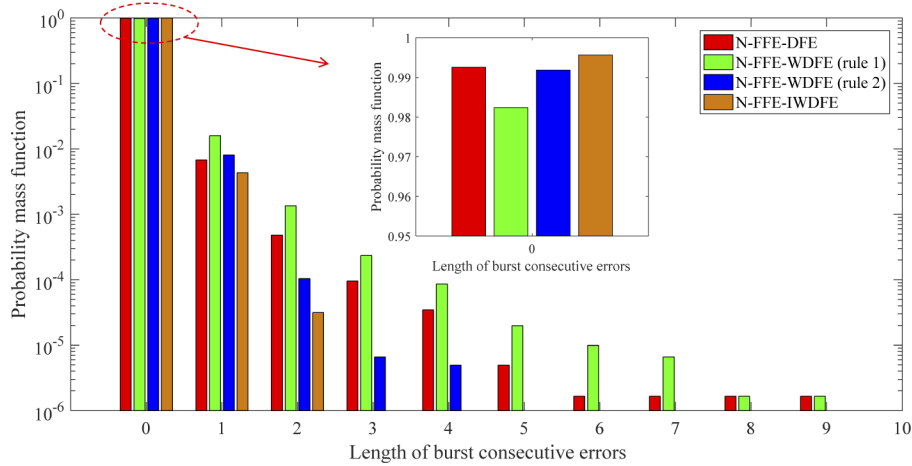


Fig. 7. Distribution of burst consecutive errors using different DFEs. All results are measured after 50-km SSMF transmission at a ROP of -10.5 dBm.

Finally, we evaluated the system transmission performance based on the N-FFE-IWDFE. Figure 8 shows the measured BER versus the ROP for 120-Gb/s PAM-4 signal transmission over 50-km SSMF. The results of the N-FFE-DFE, rule-1 and rule-2 based N-FFE-WDFEs are depicted for comparison. The BERs of rule-1 and rule-2 based N-FFE-WDFEs cannot reach the 7% HD-FEC limit of 3.8×10^{-3} due to their high percentage of symbol error. In addition, the BER performance of rule-2 based N-FFE-WDFE is better than that of N-FFE-DFE when the ROP is less than -13 dBm. Compared with N-FFE-DFE, around 1.1 dB improvement of the receiver sensitivity can be achieved by the N-FFE-IWDFE. The received eye diagrams of 120-Gb/s PAM-4 signals after 50-km transmission using N-FFE-DFE, rule-1 based N-FFE-WDFE, rule-2 based N-FFE-WDFE and N-FFE-IWDFE are shown in Figs. 8(b)-(e), respectively. The non-uniform distributed eye diagrams after 50-km transmission may be due to the time-dispersive nonlinearity as well as higher-order nonlinearity, which cannot be compensated by the nonlinear equalizers with only 2nd-order polynomial nonlinear terms used in our experiment. Thanks to the suppression of burst-error propagation and accuracy symbol decision, the eye diagram of the N-FFE-IWDFE is clearer than other three equalizers.

In order to prove the superiority in computational complexity of IWDFE, a comparison of the equalization complexity for different schemes including FFE-DFE, 3rd-order PNLE, M^L -state MLSE [30], FFE-WDFE, FFE-IWDFE, 2nd-order N-FFE-IWDFE, $(N+1)$ -symbol joint decision scheme with FFE-DFE in [8] and multiple cascaded equalization scheme including 3rd-order PNLE, FFE-WDFE and M^L -state MLSE in [26] for each PAM-4 symbol is shown in Table 2.

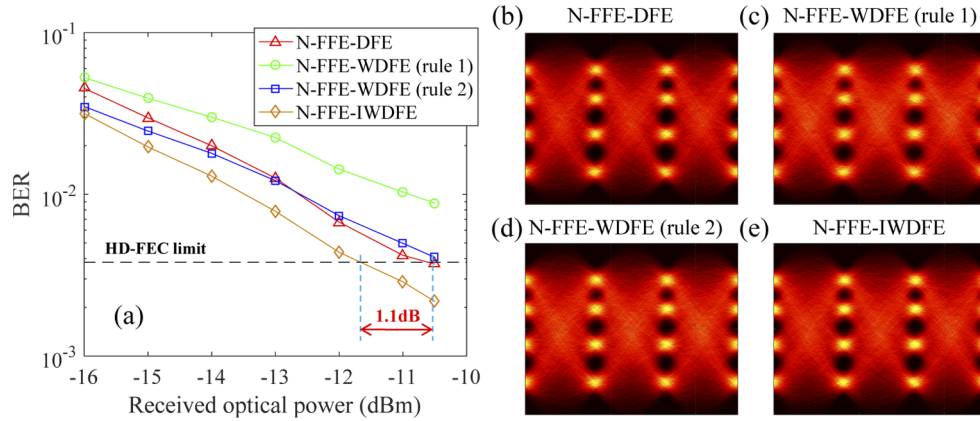


Fig. 8. (a) Measured BER versus ROP after 50-km SSMF transmission; received eye diagrams for (b) N-FFE-DFE, (c) rule-1 based N-FFE-WDFE, (d) rule-2 based N-FFE-WDFE (e) N-FFE-IWDFE at a ROP of -10.5 dBrm.

In the case of linear equalization, the computational complexity of FFE-IWDFE is much lower than that of $(N + 1)$ -symbol joint decision scheme with FFE-DFE used in [8], which grows exponentially by N . With respect to the case of nonlinear equalization using the same memory lengths, the computational complexity of 2nd-order N-FFE-IWDFE is also much lower than that of multiple cascaded equalization scheme including 3rd-order PNLE, FFE-WDFE and M^L -state MLSE in [26], in which the computational complexity of M^L -state MLSE increases exponentially with the increase of memory length L [30]. It should be noted that the equalization performance of FFE-IWDFE is superior to the conventional FFE-DFE and FFE-WDFE in reducing both the error propagation probability and percentage of errors, while containing similar computational complexity. Similar as FFE-DFE and FFE-IWDFE in [26], the FFE-IWDFE can also be combined with a MLSE or a Volterra filter to further improve its equalization performance. A further comparison of equalization performance and computational complexity among abovementioned schemes will be investigated in future study.

Table 2. Required number of real-valued multiplications per PAM-4 symbol of different equalizers.^a

Scheme	Number of real-valued multiplications
FFE-DFE	$N_1 + D_1$
3 rd -order PNLE	$Np_1 + 2Np_2 + 3Np_3$
4^L -state MLSE [30]	$O(4^{L+1})$
FFE-WDFE/ FFE-IWDFE	$N_1 + D_1 + 1$
2 nd -order N-FFE-IWDFE	$N_1 + 2N_2 + D_1 + 2D_2 + 1$
$(N + 1)$ -symbol joint decision scheme with FFE-DFE [8]	$(N_1 + D_1)(N + 1) + 2N(N + 1) + 4(4^{N+1} - 1)/3$
Multiple cascaded equalization scheme including 3 rd -order PNLE, FFE-WDFE and 4^L -state MLSE [26]	$Np_1 + 2Np_2 + 3Np_3 + N_1 + D_1 + 1 + O(4^{L+1})$

^a(N_1 and D_1 are memory lengths of FFE and DFE, respectively. N_2 and D_2 are 2nd-order nonlinear memory lengths of 2nd-order terms of the N-FFE-IWDFE. Np_1 , Np_2 and Np_3 are the linear, 2nd-order and 3rd-order memory lengths of PNLE, respectively. L is the memory length of MLSE.)

5. Conclusion

We have adopted and experimentally demonstrated an IWDFE to mitigate CD-induced power fading for C-band PAM-4 system. 2nd-order polynomial nonlinear terms have also been implemented in both FFE and IWDFE at receiver side, constructing a N-FFE-IWDFE to simultaneously equalize the CD-induced power fading and nonlinear distortions. Experimental results show that the N-FFE-IWDFE outperforms the conventional N-FFE-DFE, rule-1 and rule-2 based N-FFE-WDFEs in terms of the error propagation probability and percentage of errors. Compared with N-FFE-DFE, rule-1 and rule-2 based N-FFE-WDFEs, the N-FFE-IWDFE can significantly reduce BER, which is close to that of the EP-free N-FFE-DFE. By utilizing the N-FFE-IWDFE, 120-Gb/s PAM-4 transmission system over 50-km SSMF has been realized with the BER below 7% HD-FEC limit of 3.8×10^{-3} , achieving around 1.1-dB improvement of the receiver sensitivity over the conventional N-FFE-DFE. These results show that the IWDFE has a great potential in high-performance and low-cost IM/DD optical transmission systems.

Funding. National Key Research and Development Program of China (2018YFB1801701); National Natural Science Foundation of China (61875233, 62101602, 62105273, U1701661); The Key R&D Program of Guangdong Province (2018B030329001); Local Innovative and Research Teams Project of Guangdong Pearl River Talents Program (2017BT01X121); Open Projects Foundation of State Key Laboratory of Optical Fiber and Cable Manufacture Technology (YOFC) (SKLD1806); Science and Technology Planning Project of Guangdong Province (2019A050510039).

Disclosures. The authors declare no conflicts of interest.

Data availability. Data underlying the results presented in this paper are not publicly available at this time but may be obtained from the authors upon reasonable request.

References

1. M. Chagnon, "Optical communications for short reach," *J. Lightwave Technol.* **37**(8), 1779–1797 (2019).
2. Q. Hu, M. Chagnon, K. Schuh, F. Buchali, and H. Bülow, "IM/DD Beyond Bandwidth Limitation for Data Center Optical Interconnects," *J. Lightwave Technol.* **37**(19), 4940–4946 (2019).
3. K. Zhong, X. Zhou, J. Huo, C. Yu, C. Lu, and A. P. T. Lau, "Digital signal processing for short-reach optical communications: a review of current technologies and future trends," *J. Lightwave Technol.* **36**(2), 377–400 (2018).
4. J. Wei, T. Rahman, S. Calabrò, N. Stojanovic, L. Zhang, C. S. Xie, Z. C. Ye, and M. Kushnerov, "Experimental demonstration of advanced modulation formats for data center networks on 200 Gb/s lane rate IMDD links," *Opt. Express* **28**(23), 35240–35250 (2020).
5. IEEE 802.3bs-2017 - IEEE Standard for Ethernet Amendment 10: Media Access Control Parameters, Physical Layers, and Management Parameters for 200 Gb/s and 400 Gb/s Operation.
6. J. Wei, Q. Cheng, R. V. Pentty, I. H. White, and D. G. Cunningham, "400 Gigabit Ethernet Using Advanced Modulation Formats: Performance, Complexity, and Power Dissipation," *IEEE Commun. Mag.* **53**(2), 182–189 (2015).
7. X. Zhou, R. Urata, and H. Liu, "Beyond 1 Tb/s Intra-Data Center Interconnect Technology: IM-DD OR Coherent?" *J. Lightwave Technol.* **38**(2), 475–484 (2020).
8. X. Tang, Y. Qiao, Y. W. Chen, Y. Lu, and G. K. Chang, "Digital pre- and post-equalization for C-band 112-Gb/s PAM4 short-reach transport systems," *J. Lightwave Technol.* **38**(17), 4683–4690 (2020).
9. J. Jignesh, T. A. Eriksson, M. Chagnon, B. Corcoran, A. J. Lowery, F. Buchali, and H. Bülow, "Transmitter-side Volterra Filtering for Increased Dispersion Tolerance in 56 Gbaud PAM-4 Systems," in Proc. OFC 2018, Paper. M2C.6.
10. R. Rath, D. Clausen, S. Ohlendorf, S. Pachnicke, and W. Rosenkranz, "Tomlinson-Harashima precoding for dispersion uncompensated PAM-4 transmission with direct-detection," *J. Lightwave Technol.* **35**(18), 3909–3917 (2017).
11. N.-P. Diamantopoulos, H. Nishi, W. Kobayashi, K. Takeda, T. Kakitsuka, and S. Matsuo, "On the Complexity Reduction of the Second-Order Volterra Nonlinear Equalizer for IM/DD Systems," *J. Lightwave Technol.* **37**(4), 1214–1224 (2019).
12. J. Zhang, Z. Lin, X. Wu, J. Liu, A. P. T. Lau, C. Guo, C. Lu, and S. Yu, "Low-complexity sparse absolute-term based nonlinear equalizer for C-band IM/DD systems," *Opt. Express* **29**(14), 21891–21901 (2021).
13. N. Eiselt, J. Wei, H. Griesser, A. Dochhan, M. H. Eiselt, J.-P. Elbers, J. J. V. Olmos, and I. T. Monroy, "Evaluation of real-time 8×56.25 Gb/s (400G) PAM-4 for inter-data center application over 80 km of SSMF at 1550 nm," *J. Lightwave Technol.* **35**(4), 955–962 (2017).
14. Z. Wan, J. Li, L. Shu, S. Fu, Y. Fan, F. Yin, Y. Zhou, Y. Dai, and K. Xu, "64-Gb/s SSB-PAM4 transmission over 120-km dispersion-uncompensated SSMF with blind nonlinear equalization, adaptive noise-whitening postfilter and MLSD," *J. Lightwave Technol.* **35**(23), 5193–5200 (2017).
15. J. Lee, N. Kaneda, and Y. K. Chen, "112-Gbit/s Intensity-Modulated Direct-Detect Vestigial-Sideband PAM4 Transmission over an 80-km SSMF Link," in ECOC 2016, Paper. M.2.D.3.

16. Q. Zhang, N. Stojanovic, J. Wei, and C. Xie, "Single-lane 180 Gb/s DBPAM-4-signal transmission over an 80 km DCF-free SSMF link," *Opt. Lett.* **42**(4), 883–886 (2017).
17. A. Mecozzi, C. Antonelli, and M. Shtaif, "Kramers–Kronig coherent receiver," *Optica* **3**(11), 1220–1227 (2016).
18. X. Chen, C. Antonelli, S. Chandrasekhar, G. Raybon, A. Mecozzi, M. Shtaif, and P. Winzer, "Kramers–Kronig Receivers for 100-km Datacenter Interconnects," *J. Lightwave Technol.* **36**(1), 79–89 (2018).
19. X. Tang, S. Liu, Z. Sun, H. Cui, X. Xu, J. Qi, M. Guo, Y. Lu, and Y. Qiao, "C-band 56-Gb/s PAM4 transmission over 80-km SSMF with electrical equalization at receiver," *Opt. Express* **27**(18), 25708–25717 (2019).
20. H. Xin, K. Zhang, L. Li, H. He, and W. Hu, "50 Gbps PAM-4 Over Up to 80-km Transmission With C-Band DML Enabled by Post-Equalizer," *IEEE Photonics Technol. Lett.* **32**(11), 643–646 (2020).
21. Q. Hu, K. Schuh, M. Chagnon, F. Buchali, S. T. Le, and H. Bülow, "50 Gb/s PAM-4 Transmission Over 80-km SSMF Without Dispersion Compensation," in *ECOC 2018*, 1–3.
22. H. Xin, K. Zhang, D. Kong, Q. Zhuge, Y. Fu, S. Jia, W. Hu, and H. Hu, "Nonlinear tomlinson-harashima precoding for direct-detected double sideband pam-4 transmission without dispersion compensation," *Opt. Express* **27**(14), 19156–19167 (2019).
23. R. F. Fischer, *Precoding and signal shaping for digital transmission* (John Wiley & Sons, 2005).
24. H. Wang, J. Zhou, D. Guo, Y. Feng, W. Liu, C. Yu, and Z. Li, "Adaptive Channel-Matched Detection for C-Band 64-Gbit/s Optical OOK System over 100-km Dispersion-Uncompensated Link," *J. Lightwave Technol.* **38**(18), 5048–5055 (2020).
25. J. Zhou, H. Wang, Y. Feng, W. Liu, S. Gao, C. Yu, and Z. Li, "Processing for dispersive intensity-modulation and direct-detection fiber-optic communications," *Opt. Lett.* **46**(1), 138–141 (2021).
26. J. Zhou, C. Yang, D. Wang, Q. Sui, H. Wang, S. Gao, Y. Feng, W. Liu, Y. Yan, J. Li, C. Yu, and Z. Li, "Burst-Error-Propagation Suppression for Decision-Feedback Equalizer in Field-Trial Submarine Fiber-Optic Communications," *J. Lightwave Technol.* **39**(14), 4601–4606 (2021).
27. J. Palicot, "A weighted decision feedback equalizer with limited error propagation," in *IEEE International Conference on Communications 2000*, 377–381.
28. J. Palicot and A. Goupil, "Performance analysis of the weighted decision feedback equalizer," *Signal Process.* **88**(2), 284–295 (2008).
29. A. Zaknich, *Principles of Adaptive Filters and Self-Learning Systems*, Springer, Berlin, Germany, 2006.
30. W. H. Mow, "Maximum likelihood sequence estimation from the lattice viewpoint," *IEEE Trans. Inf. Theory* **40**(5), 1591–1600 (1994).